Control Relevant Identification for Third-Order Volterra Systems: A Polymerization Case Study

Abhishek S. Soni and Robert S. Parker
Department of Chemical and Petroleum Engineering
University of Pittsburgh, 1249 Benedum Hall, Pittsburgh, PA 15261
rparker@pitt.edu

Abstract

In this work the problem of identifying third-order Volterra models from input-output process data is addressed. The identification problem involves the rational design of input sequences that exploit the Volterra model structure. The criterion used to measure the model fitness is the minimization of the prediction error variance (PEV). Explicit estimators that utilize plant-friendly input sequences for the identification of bias, linear, nonlinear diagonal, and third-order sub-diagonal kernels are presented. As an application of this technique, an isothermal polymerization reactor case study is considered; it was found that the third-order Volterra model does an efficient job of capturing the nonlinear reactor behavior.

Keywords: empirical model identification, input sequence design, Volterra series, polymerization reactor

1 Introduction

The increased emphasis on maintaining productivity with sustained product quality has imposed strict requirements on controller performance. For a model based control scheme there is a direct link between model quality and theoretically achievable controller performance [1]. Consequently, controllers based on nonlinear models are needed as they provide higher quality control performance over a wider manipulated variable range than controllers based on linear models. One of the key impediments to the practical application of nonlinear model based controllers is the availability of suitable nonlinear models [2]. In this regard, a number of researchers have focused on developing nonlinear models from first-principles [3], [4]. An advantage of fundamental models is that since they are based on the underlying physics of the problem, they have parameters with physical correspondence. Due to the physical insight provided by these models, they can be used with confidence beyond the operating range in which they were developed provided the quality of the parameter estimates is good. However, these models are time-consuming to develop and often have a very high state dimension and a large number of parameters that need to be identified from process data. This complexity in the system model manifests directly in the controller design and implementation which may be computationally intensive. Furthermore, the optimization problem that is solved in nonlinear model predictive control (NMPC) is now a nonlinear programming problem (NLP) in contrast to the more tractable convex quadratic program (QP) solved for linear MPC.

An alternative to the use of first-principles models is to use empirical or black-box modeling techniques. Here a mathematical representation is chosen and the model parameters are calculated to best capture the input-output behavior of the process. Among the commonly used model frameworks are artificial neural networks (ANN) and nonlinear moving average with exogenous input models, either with (NARMAX) or without (NMAX) auto-regressive terms. Since these models are based purely on input-output data they do not capture the underlying physics of the process. However they are often much easier to develop; as a testimony to their appeal, a vast majority of industrial MPC controllers employ empirical dynamic models [2]. This makes system identification from plant data a practical and relevant problem. However, in most cases linear empirical models are used for controller design and this may affect the performance when the underlying physical process is nonlinear. Thus there is a need to identify nonlinear models quickly for processes that warrant a nonlinear controller.

The choice of the input signal is one of the primary design elements in a system identification scheme. The chosen input sequence should be persistently exciting, *i.e.* it should be able to elicit sufficient output response in order to identify the parameters in the model structure. It is also desired to be plant-friendly [5], such that it provides enough excitation to identify the model parameters without causing excessive actuator movement, and without causing the plant to deviate significantly from its nominal operating point. The metric used to analyze plant-friendliness in this work is the friendliness factor f given as [5]:

$$f = 100\left(1 - \frac{n_t}{N-1}\right) \tag{1}$$

Here, N is the total sequence length whereas n_t is the total number of level transitions. An alternative approach is to use frequency domain information whereby multisine signals are employed with a goal of minimizing the crest-factor (ratio of the ℓ_∞ norm of the input to its ℓ_2 norm). A low crest factor signifies that most of the values of the input sequence are distributed around its extreme ends. Minimization of

the crest factor improves the signal to noise ratio of the output thereby making the input sequence plant friendly [6]. However, in the context of this work the discussion is limited to time domain input signals with a goal of minimizing actuator wear due to frequent transitions in the input sequence.

2 Third-order Volterra models

The general form of the Volterra model is given as,

$$y(k) = h_0 + \sum_{i=1}^{N}\sum_{j_1=1}^{M} \cdot\cdot \sum_{j_N=1}^{M} h_i(j_1,..,j_N)u(k-j_1)\cdot\cdot u(k-j_N) \tag{2}$$

In this equation, N is the model order and M is the model memory, the duration over which the past inputs have an effect on the current output, $y(k)$. The Volterra model kernels are given by $h_i(j_1,...,j_N)$, and the identification problem involves determining the values of these kernels. The Volterra model structure is capable of capturing a variety of nonlinear systems behavior [7],[8]. An example is the ability to capture asymmetric output responses to symmetric changes in the input; this behavior is shown by many chemical engineering systems including reactors and distillation columns. Furthermore, the Volterra model returns the linear finite impulse response (FIR) model for $N = 1$ in (2). Thus the Volterra model structure can be considered as a nonlinear extension of the FIR model thereby facilitating its use in on-line applications. One disadvantage of this structure is the number of parameters that must be estimated as the model order increases. This factor has limited the widespread use of higher-order Volterra models for practical applications. In this work, it is shown that by judiciously exploiting the model structure, input sequences can be tailored so as to simplify the task of, and minimize the data requirements for, identifying the parameters for a third-order Volterra model. The third-order Volterra model is first decomposed in the following manner [5]:

$$\hat{y}(k) = h_0 + L(k) + D(k) + S(k) + O(k) \tag{3}$$

$$\begin{aligned}
L(k) &= \sum_{i=1}^{M} h_1(i)u(k-i) \\
D(k) &= \sum_{i=1}^{M} h_2(i,i)u^2(k-i) + \sum_{i=1}^{M} h_3(i,i,i)u^3(k-i) \\
S(k) &= 3\sum_{i=1}^{M}\sum_{j=1}^{i-1} h_3(i,i,j)u^2(k-i)u(k-j) \\
&\quad + 3\sum_{i=1}^{M}\sum_{j=1}^{i-1} h_3(i,j,j)u(k-i)u^2(k-j) \\
O(k) &= 2\sum_{i=1}^{M}\sum_{j=1}^{i-1} h_2(i,j)u(k-i)u(k-j) + \\
&\quad 6\sum_{i=1}^{M}\sum_{j=1}^{i-1}\sum_{\ell=1}^{j-1} h_3(i,j,\ell)u^2(k-i)u(k-j)u(k-\ell)
\end{aligned}$$

Here, L, D, S, and O represent the linear, nonlinear diagonal, third-order sub-diagonal, and nonlinear off-diagonal terms, respectively. The Volterra model can be assumed symmetric without loss of generality [9]. Symmetry in the third-order term can be visualized with respect to the main diagonal.

2.1 Third-order Volterra model Identification

The identification of the Volterra model coefficients is carried out based on the decomposition presented in (3). As a metric to analyze model fitness, consider the third-order Prediction Error Variance expression:

$$\begin{aligned}
\sigma_p^2 &= \sigma_0^2 + \sigma_u^2\sum_{i=1}^{M}\delta_1^2(i) + (\kappa+2)\sigma_u^4\sum_{i=1}^{M}\delta_2^2(i,i) \\
&\quad + 2\sigma_u^4\sum_{i=1}^{M}\sum_{j=1}^{i-1}\delta_2^2(i,j) + (m_6 - \frac{m_4^2}{\sigma_u^2})\sum_{i=1}^{M}\delta_3^2(i,i,i) \\
&\quad + 9(\kappa+2)\sigma_u^6\sum_{i=1}^{M}\sum_{j=1}^{M}\delta_3^2(i,j,j) \\
&\quad + 6\sigma_u^6\sum_{i=1}^{M}\sum_{j\neq i}^{M}\sum_{\ell\neq j\neq i}^{M}\delta_3^2(i,j,\ell)
\end{aligned} \tag{4}$$

The first term represents the bias term whereas the second, third, and fourth terms describe the contributions due to the coefficient errors in the linear, second-order diagonal, and the second-order off-diagonal terms. The last three terms represent the third-order diagonal, third-order sub-diagonal and the third-order off-diagonal terms, respectively. The input sequences designed in the present work are based on the structure and coefficients of the terms in (3) and (4). Thus, an input-sequence which makes the coefficient $\left(m_6 - \frac{m_4^2}{\sigma_u^2}\right)$ large would be a candidate to identify the third-order diagonal kernel. For the third-order sub-diagonal terms, if an input sequence is designed such that no more than two points have non-zero values within the model memory M then the third-order off-diagonal terms would be zero identically (according to (3)). Furthermore, the ratio of the coefficient of the third-order sub-diagonal term to that of the second-order off-diagonal term is:

$$\frac{C_{3SD}}{C_{2OD}} = 4.5(\kappa+2)\sigma_u^2 \tag{5}$$

Thus, a sequence with a high kurtosis and a high variance could selectively excite the third-order sub-diagonal terms and render the effects of the second-order off-diagonal terms relatively insignificant. Thus, the identification algorithmfor third-order Volterra models is as follows:

Identification Algorithm

First, the bias, linear, and nonlinear diagonal parameters are estimated using a four-pulse, five-level, $4M+4$ length sequence. Next, a $57M$ length tailored sequence is used to excite the system and residuals are calculated by subtracting off the bias, linear, and nonlinear diagonal contributions.

Third-order sub-diagonal coefficients are estimated from these residuals. Finally the second and third order off-diagonal terms can be estimated using a cross-correlation technique building on the results presented in [5].

2.2 Estimation of bias, linear, and nonlinear diagonal parameters

The identification of the bias, linear, and nonlinear diagonal parameters is carried out first in order to take advantage of tailored input sequences that selectively excite these parameters. Furthermore, since the diagonal parameters are involved in the calculation of all of the other parameters, an accurate estimate of the diagonal terms at the beginning ensures better estimates for the subsequent parameters. Akin to the results of [10], a $4M+4$ length deterministic input sequence is used to estimate the bias, linear, and diagonal parameters.

$$u(k) = \begin{cases} \gamma_1 & k = 0 \\ 0 & 1 \le k \le M \\ -\gamma_1 & k = M+1 \\ 0 & M+2 \le k \le 2M+1 \\ \gamma_2 & k = 2M+2 \\ 0 & 2M+3 \le k \le 3M+2 \\ -\gamma_2 & k = 3M+3 \\ 0 & 3M+4 \le k \le 4M+3 \end{cases} \tag{6}$$

This sequence ensures that the contributions due to the nonlinear sub-diagonal and off-diagonal terms are zero identically, $(u(k-i)u(k-j) = 0 \ \ \forall i \neq j \ \ (i,\ j \ \le M))$. The parameters γ_1 and γ_2 are selected such that $\gamma_2 > \gamma_1$. This is done in order to facilitate sufficient excitation of the model nonlinearities. In addition, the placement of the smaller pulse before the larger pulse guarantees that any residual error from the large pulse response does not corrupt the small pulse output data. For a value of $\gamma_1 = 5.6$ and $\gamma_2 = 56$, this sequence has a friendliness factor of 93%. Furthermore, the value of the coefficient $\left(m_6 - \frac{m_4^2}{\sigma_u^2}\right)$ for this sequence is $712,570$ which ensures sufficient excitation. Assuming

$$y(k) = \hat{y}(k) + e(k) \quad \text{for } k = 0,\ 1\ ,\ \ldots\ ,\ 4M+3$$

one can obtain estimates for the linear and diagonal kernels that minimize the following sum-squared prediction error:

$$J = \sum_{k=0}^{4M+3} e(k)^2 = \sum_{k=0}^{4M+3} \{y(k) - \hat{y}(k)\}^2 \tag{7}$$

In this equation $e(k)$ is a zero-mean prediction error sequence due to measurement errors in the data-set $y(k)$ and any plant-model mismatch, and $\hat{y}(k)$ is the model prediction with the input sequence given in (6). Applying the condition,

$$\frac{\partial J}{\partial h_n} = 0 \qquad n = 0,1,2,3. \tag{8}$$

and simultaneously solving the equations for $\frac{\partial J}{\partial h_1} = 0$ and $\frac{\partial J}{\partial h_3} = 0$, estimators for the linear and the third-order diagonal kernels are obtained. This is a departure from [5] where the estimator $h_1(k)$ was calculated independently. Since the current sequence identifies a third-order Volterra model, the estimators for h_1 and h_3 are interdependent and must be calculated simultaneously. After significant algebra, the odd-order estimators are as follows:

$$\begin{aligned} h_1(k) &= \frac{n_1(k)}{d_{odd}(k)} \qquad (9) \\ n_1(k) &= \frac{\gamma_1^6+\gamma_2^6}{\gamma_1^4+\gamma_2^4}\Big\{\frac{\gamma_1}{2(\gamma_1^2+\gamma_2^2)}\{y(k)-y(k+M+1)\} \\ &\quad +\frac{\gamma_2}{2(\gamma_1^2+\gamma_2^2)}\{y(k+2M+2)-y(k+3M+3)\}\Big\} \\ &\quad -\frac{\gamma_1^4+\gamma_2^4}{\gamma_1^2+\gamma_2^2}\Big\{\frac{\gamma_1^3}{2(\gamma_1^4+\gamma_2^4)}\{y(k)-y(k+M+1)\} \\ &\quad +\frac{\gamma_2^3}{2(\gamma_1^4+\gamma_2^4)}\{y(k+2M+2)-y(k+3M+3)\}\Big\} \\ d_{odd}(k) &= \frac{\gamma_1^6+\gamma_2^6}{\gamma_1^4+\gamma_2^4} - \frac{\gamma_1^4+\gamma_2^4}{\gamma_1^2+\gamma_2^2} \end{aligned}$$

$$\begin{aligned} h_3(k) &= \frac{n_3(k)}{d_{odd}(k)} \qquad (10) \\ n_3(k) &= \Big\{\frac{\gamma_1^3}{2(\gamma_1^4+\gamma_2^4)} - \frac{\gamma_1}{2(\gamma_1^2+\gamma_2^2)}\Big\}\{y(k)-y(k+M+1)\} \\ &\quad +\Big\{\frac{\gamma_2^3}{2(\gamma_1^4+\gamma_2^4)} - \frac{\gamma_2}{2(\gamma_1^2+\gamma_2^2)}\Big\}\{y(k+2M+2) \\ &\quad -y(k+3M+3)\} \end{aligned}$$

Similarly, solving for $\frac{\partial J}{\partial h_0} = 0$ and $\frac{\partial J}{\partial h_2} = 0$ simultaneously, the bias term and the second-order diagonal kernel estimators are obtained. These are given as:

$$\begin{aligned} h_0 &= \frac{n_0}{d_0} \qquad (11) \\ n_0 &= \frac{\gamma_1^2}{2(\gamma_1^4+\gamma_2^4)}\sum_{k=1}^{M}\{y(k)+y(k+M+1)\} \\ &\quad +\frac{\gamma_2^2}{2(\gamma_1^4+\gamma_2^4)}\sum_{k=1}^{M}\{y(k+2M+2)+y(k+3M+3)\} \\ &\quad -\frac{1}{2(\gamma_1^2+\gamma_2^2)}\sum_{k=0}^{4M+3} y(k) \\ d_0 &= M\frac{\gamma_1^2+\gamma_2^2}{\gamma_1^4+\gamma_2^4} - \frac{2M+2}{\gamma_1^2+\gamma_2^2} \end{aligned}$$

$$\begin{aligned} h_2(k) &= \frac{\gamma_1^2}{2(\gamma_1^4+\gamma_2^4)}\{y(k)+y(k+M+1)\} \\ &\quad +\frac{\gamma_2^2}{2(\gamma_1^4+\gamma_2^4)}\{y(k+2M+2)+y(k+3M+3)\} \\ &\quad -\frac{\gamma_1^2+\gamma_2^2}{\gamma_1^4+\gamma_2^4}h_0 \qquad (12) \end{aligned}$$

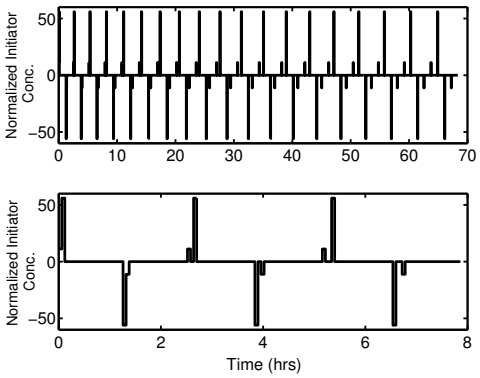

Figure 1: Top — Input sequence used for sub-diagonal identification. The levels used are $\lambda_1 = 11.2$ and $\lambda_2 = 56$. Bottom — Zoom of the plot over the first 8 hours to show increasing pulse separation with time.

2.3 Estimation of sub-diagonal parameters

One CSRS input sequence which is plant-friendly in valve usage ($f = 94\%$) is shown in Figure 1. A short length of the sequence is also shown in order to highlight its behavior. For this sequence the ratio given by (5) is $13,102$ which ensures selective excitation of the third-order sub-diagonal terms. In order to derive the sub-diagonal estimator equations, an approach similar to that used for the derivation of the bias, linear, and the diagonal estimators is used. The calculation here is shown for just one sub-unit of the sequence but it can be generalized to the entire sequence length. The only difference is that in subsequent sub-units of the input sequence there is a gap between the two pulses. This gap length increases by one with increasing sub-units, and it is employed to ensure the tailored excitation of all of the sub-diagonal parameters. The first sub-unit of the input sequence is given as:

$$u(k) = \begin{cases} \lambda_1 & k = 1 \\ \lambda_2 & k = 2 \\ 0 & 3 \leq k \leq M+1 \\ -\lambda_2 & k = M+2 \\ -\lambda_1 & k = M+3 \\ 0 & M+4 \leq k \leq 2M+2 \end{cases} \tag{13}$$

Applying this to the system of interest and removing the bias, linear, and nonlinear diagonal contributions, recovers the residual $z(k)$. The estimates for the third-order sub-diagonal coefficients can be obtained by minimizing the following sum-squared prediction error:

$$J_{sd} = \sum_{k=1}^{2M+2} \{z(k) - \hat{z}(k)\}^2 \tag{14}$$

Solving for $\frac{\partial J_{sd}}{\partial h_3(i,j,j)} = 0$ and $\frac{\partial J_{sd}}{\partial h_3(i,i,j)} = 0$ simultaneously, the estimators for the third-order sub-diagonals are as follows:

$$\begin{aligned} h_3(i,j,j) &= \frac{\alpha_1}{\alpha_1^2 - \alpha_2^2} z(k+2) + \frac{\alpha_1}{\alpha_2^2 - \alpha_2^2} z(k+M+3) \\ h_3(i,i,j) &= \frac{-\alpha_2}{\alpha_1^2 - \alpha_2^2} z(k+2) + \frac{-\alpha_1}{\alpha_1^2 - \alpha_2^2} z(k+M+3) \end{aligned}$$

$$\begin{aligned} \alpha_1 &= \lambda_1^2 \lambda_2 \\ \alpha_2 &= \lambda_2^2 \lambda_1 \\ k &= 1,\ 2,\ \ldots M-1 \end{aligned} \tag{15}$$

This calculation is then carried out for the entire length of the sequence, allowing the estimation of $h_3(i,j,j)$ and $h_3(i,i,j)\ \forall\ i,j$ such that $1 \leq i,j \leq M$.

3 Case Study: A Polymerization Reactor

In order to test the effectiveness of the algorithm developed in the previous section, the isothermal free-radical polymerization of methyl-methacrylate using azo-bis-isobutyronitrile as an initiator and toluene as a solvent [11] is treated as the "real" system. A detailed description of the system has been previously published [12]. The system equations are given as,

$$\begin{aligned} \dot{x}_1 &= 60 - 10x_1 - 2.45684 x_1 \sqrt{x_2} \\ \dot{x}_2 &= 80u - 10.1022 x_2 \\ \dot{x}_3 &= 0.0024121 x_1 \sqrt{x_2} + 0.112184 x_2 - 10 x_3 \\ \dot{x}_4 &= 245.979 x_1 \sqrt{x_2} - 10 x_4 \\ y &= \frac{x_4}{x_3} \end{aligned} \tag{16}$$

In this system the output y is the number average molecular weight (NAMW) of the polymer whereas the input u is the initiator flow-rate. The nominal operating point is selected as the mid-point of the operation range of the reactor and is given in Table 1. The system was converted to deviation

Table 1: Nominal operating point

Variable	Nominal Value	Units
x_{10}	5.12796	$kmol/m^3$
x_{20}	0.4791035	$kmol/m^3$
x_{30}	0.00623093	$kmol/m^3$
x_{40}	87.308673	kg/m^3
u_0	0.0605	m^3/h
y_0	14012	$kg/kmol$

form, and the input and output were scaled as in [5]:

$$\begin{aligned} v &= \frac{u - u_0}{0.001} \\ \tilde{y} &= \frac{y - y_0}{100} \end{aligned} \tag{17}$$

Carlemann linearization of the nonlinear system [9], truncated to third-order terms returned the following bilinear system in state-space form:

$$\begin{aligned} \dot{\tilde{q}} &= A\tilde{q} + N\tilde{q}v + Bv \\ \tilde{y} &= C\tilde{q} \end{aligned} \tag{18}$$

Here $\tilde{q}$ represents the states of the bilinear system. A plot of the system response to step-changes of magnitude $v = \pm 30$ are shown in Figure 2. The corresponding system responses from the second- and third-order Carlemann linearized

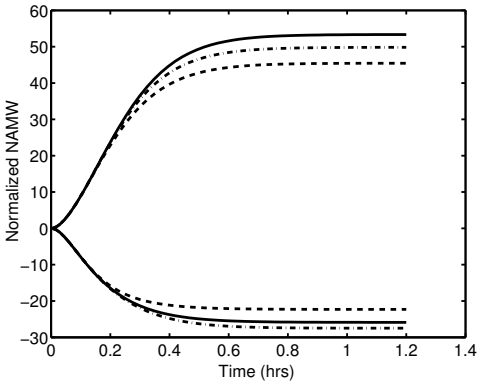

Figure 2: Plot of the response to a step-change of ± 30 in $v\,(m^3/h)$. Nonlinear model (—), Carlemann linearized model truncated to second-order $(--)$, Carlemann linearized model truncated to the third-order $(-\cdot-)$

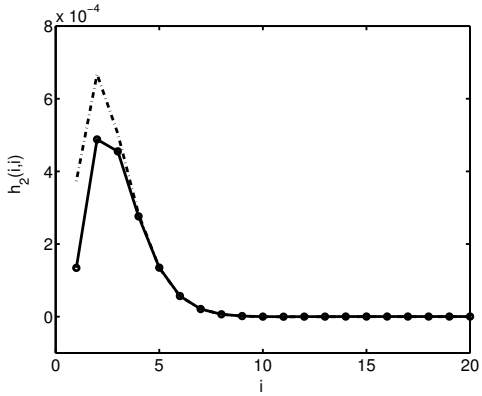

Figure 3: A comparison of the analytically calculated $(-\cdot-)$ with the identified (2M+2 length) $(-\bullet-)$ second-order diagonal kernel.

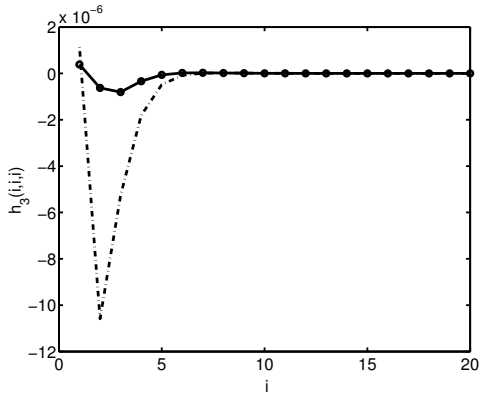

Figure 4: A comparison of the analytically calculated $(-\cdot-)$ with the identified $(-\bullet-)$ third-order diagonal kernel.

models are also shown. Since the third-order Carlemann linearized model captures the system response better than the second-order model, all further analysis is carried out using the third-order Carlemann linearized model.

Finally, the bilinear state-space system was discretized using the fourth-order Runge-Kutta algorithm. A sampling time (Δt) of 0.06 *hr* and model-memory M of 20, were selected to allow comparison with [5]. From the discretized equations, the Volterra kernels for the system were calculated analytically [9]. A third-order Volterra model was thus obtained, which is used to test the effectiveness of the identification algorithm vis-a-vis the real system.

3.1 Results

The system output profiles, generated using the input sequences for the linear, and nonlinear diagonal, and the sub-diagonal estimation, were used to estimate the kernels using the Algorithm from Section 2.1. Table 2 shows the comparison of the identified kernel estimates with the analytically derived kernels. Plots that show the comparison of the identified and analytical second-order (Figure 3) and third-order (Figure 4) diagonal kernels are also shown.

Table 2: Error summary for the identification results, with values as sum-squared coefficient error.

Error	Algorithm 1
Linear	3.69×10^{-6}
2^{nd}-Order Diagonal $(4M+4)$	1.47×10^{-7}
2^{nd}-Order Diagonal $(2M+2)$	9.16×10^{-8}
3^{rd}-Order Diagonal	1.22×10^{-10}
3^{rd}-Order Sub-diagonal	2.95×10^{-9}

It is observed that the identification algorithm does an excellent job of identifying the linear Volterra model kernels as is evident from the low value of the sum-squared coefficient error. The identification of the second-order diagonal kernel was also carried out using only the latter half of the $4M+4$ sequence (*i.e.* the $2M+2$ length sequence with pulses of magnitude $\pm$ 56). This second-order diagonal kernel is shown in Figure 3. The improvement in this result over that obtained from using the full sequence is probably due to insufficient excitation of the second-order diagonal kernel by the low-magnitude pulses. Although this difference between the two values does not appear significant at a first glance, any error at this stage is propagated into the identification of the third-order sub-diagonal coefficients. For the third-order diagonal kernels the identified kernel captures the qualitative behavior, *i.e.* a parabolic dip initially followed by a plateau. However, it does not capture the "minimum" of this dip, quantitatively. As in the second-order case, a re-evaluation of γ_1 may improve the accuracy of the estimator. For both the second- and third-order kernels the saturation behavior with increasing i is adequately represented.

The third-order sub-diagonal coefficients were identified using the input sequence in Figure 1, with $\lambda_1 = 11.2$ and $\lambda_2 = 56$. A mesh plot that shows a comparison of the identified and analytical third-order sub-diagonal kernels is

shown in Figure 5. In this case as well, the qualitative

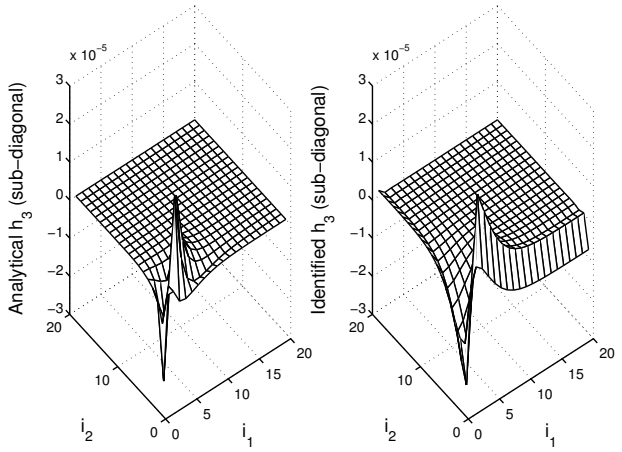

Figure 5: Mesh plot of the analytical (left) and the identified (right) third-order sub-diagonals.

behavior of the kernel is captured. Quantitatively, the accuracy of the third-order sub-diagonal appears good, but the graphical comparison in Figure 5 shows a systematic error in the early (small index) coefficients. The kernel error can be attributed to the quality of residuals that are obtained from subtracting the contribution of the diagonal kernels from the system output. Errors in the identification of the nonlinear diagonal kernels are now magnified in the calculation of the third-order sub-diagonal kernels. In order to check if this was indeed the case, the identification was done without using the residuals, *i.e.* by using the output from the theoretical third-order sub-diagonal kernel for identification. The sum-squared error obtained in this case was 3.19×10^{-41}, thereby confirming the validity of the third-order sub-diagonal estimators in (15). It also highlights the significant impact of errors in nonlinear diagonal kernel estimation on the third-order sub-diagonal estimates.

4 Summary

In this work, the identification of a third-order Volterra model was considered. Tailored input sequences were designed based on the PEV expression and these sequences adequately exploited the Volterra model structure. The estimation of the bias, linear, and nonlinear diagonal parameters was carried out using a four pulse sequence, and the third-order sub-diagonal parameters were estimated using a novel sequence designed to preferentially excite the third-order sub-diagonal terms over the second-order off-diagonal terms. Thus a systematic and rational approach towards identification of third-order Volterra models was presented using plant-friendly input sequences.

It is expected that improvements in input sequence design, with respect to pulse magnitude and spacing, may lead to improvements in diagonal kernel coefficient estimation. Furthermore, it may be possible to shorten the sequence length (and hence, time required) for sub-diagonal kernel estimation. These topics, as well as a comparison to cross-correlation techniques are areas of ongoing work.

5 Acknowledgments

Support for this work was provided by the National Science Foundation (CAREER, CTS #0134129).

References

[1] M. Morari and E. Zafiriou. *Robust Process Control*. Prentice-Hall, Englewood Cliffs, NJ, 1989.

[2] S. J. Qin and T. A. Badgwell. An overview of nonlinear MPC applications. In F. Allgower and A. Zheng, editors, *Nonlinear Model Predictive Control: Assessment and Future Directions*. Birkhauser, 1999.

[3] A. M. Zamamiri, Y. Zhang, M. A. Henson, and M. A. Hjortsø. Dynamics analysis of an age distribution model of oscillating yeast cultures. *Chem. Eng. Sci.*, 57:2169–2181, 2002.

[4] T. J. Crowley, E. S. Meadows, E. Kostoulas, and F. J. Doyle III. Control of particle size distribution described by a population balance model of semibatch emulsion polymerization. *J. Proc. Control*, 10:419–432, 2000.

[5] R. S. Parker, D. Heemstra, F. J. Doyle III, R. K. Pearson, and B. A. Ogunnaike. The identification of nonlinear models for process control using tailored "plant–friendly" input sequences. *J. Proc. Control*, 11, Sp. Issue SI:237–250, 2001.

[6] M. W. Braun, R. Ortiz-Mojica, and D. E. Rivera. Application of minimum crest factor multisinusoidal signals for "plant-friendly" identification of nonlinear process systems. *Control Engineering Practice*, 10(3):301–313, March 2002.

[7] F. J. Doyle III, B. A. Ogunnaike, and R. K. Pearson. Nonlinear model-based control using second order Volterra models. *Automatica*, (31):697–714, 1995.

[8] C. Seretis and E. Zafiriou. Nonlinear dynamical system identification using reduced Volterra models with generalized orthonormal basis functions. In *Proc. American Control Conf.*, pages 3042–3046, Albuquerque, NM, 1997.

[9] W. J. Rugh. *Nonlinear System Theory - The Volterra/Wiener Approach*. The Johns Hopkins University Press, Baltimore, MD, 1981.

[10] J. A. Florian and R. S. Parker. A nonlinear data–driven approach to type I diabetic patient modeling. 15th IFAC World Congress on Automatic Control. IFAC, 2002.

[11] J. P. Congalidis, J. R. Richards, and W. H. Ray. Feedforward and feedback control of a solution copolymerization reactor. *AIChE J.*, 35(6):891–907, 1989.

[12] B. R. Maner, F. J. Doyle III, B. A. Ogunnaike, and R. K. Pearson. Nonlinear model predictive control of a multivariable polymerization reactor using second order volterra models. *Automatica*, 32:1285–1302, 1996.